

The time-dependent generalized active space configuration interaction approach to correlated ionization dynamics of diatomic molecules

This content has been downloaded from IOPscience. Please scroll down to see the full text.

2016 J. Phys.: Conf. Ser. 696 012008

(<http://iopscience.iop.org/1742-6596/696/1/012008>)

View the [table of contents for this issue](#), or go to the [journal homepage](#) for more

Download details:

IP Address: 134.245.67.171

This content was downloaded on 20/04/2016 at 08:57

Please note that [terms and conditions apply](#).

The time-dependent generalized active space configuration interaction approach to correlated ionization dynamics of diatomic molecules

S Bauch¹, H R Larsson², C Hinz¹ and M Bonitz¹

¹ Institute for Theoretical Physics and Astrophysics, Christian-Albrechts-Universität Kiel,
24098 Kiel, Germany

² Institute for Physical Chemistry, Christian-Albrechts-Universität Kiel, 24098 Kiel, Germany

E-mail: ¹ bauch@theo-physik.uni-kiel.de

Abstract. In this contribution, we review the time-dependent generalized-active-space configuration interaction (TD-GAS-CI) approach to the photoionization dynamics of atoms and molecules including electron correlation effects. It is based on the configuration interaction (CI) expansion of the many-body wave function and the restriction of the determinantal space to a reduced subspace. For its numerically efficient application to photoionization, a partially-rotated basis set is used which adopts features of a localized basis with a good reference description and a grid representation for escaping wave packets. After reviewing earlier applications of the theory, we address the strong-field ionization of a one-dimensional model of the four-electron LiH molecule using TD-GAS-CI and demonstrate the importance of electron-electron correlations in the ionization yield for different orientations of the molecule w.r.t the peak of the linearly polarized laser field. A pronounced orientation-dependent variation of the yield with the pulse duration and the level of considered electron-electron correlations is observed.

1. Introduction

With the emergence of ultrashort and strong laser pulses in the femtosecond and subfemtosecond regimes [1], a time-dependent theory for electron dynamics with the ability of treating strong fields and electron correlations is needed. Among the processes are the time-resolved observation of post-collision interaction [2, 3], time-delays in photoionization [4], the time-resolved observation of strong-field tunneling [5], and many more. See also the review articles [6, 7].

Often, only numerically costly methods are able to describe the ultrafast motion of the interacting electrons in the external fields. Pioneering work was based on the numerical solution of the time-dependent Schrödinger equation (TDSE) in the context of strong-field processes, e.g. [8, 9], for one-electron systems. Despite the tremendous evolution of computing architectures over the past decades, the numerical solution of the TDSE still remains a challenging task for extended systems with more than one active electron and is limited to helium, H₂ and similar systems, e.g., [10, 11, 12]. Therefore, approximative methods are inevitable. Perturbation theory in the electrical field of the excitation is extremely successful by considering the fully-correlated ground-state wave function for calculating spectra, but not applicable to the high-intensity or time-resolved regime by construction. The alternative approach is the approximative



Content from this work may be used under the terms of the [Creative Commons Attribution 3.0 licence](#). Any further distribution of this work must maintain attribution to the author(s) and the title of the work, journal citation and DOI.

treatment of the electron interaction. Within a wave-function based perspective, this leads to the concept of configuration interaction (CI) and self-consistent-field (SCF) methods, see [13] for a review. Time-dependent methods emerging from the latter are the widely applied multi-configurational time-dependent Hartree-Fock (MC-TDHF) theory, e.g. [14, 15, 16] and time-dependent restricted and complete active space (TD-R/CAS) SCF methods [17, 18, 19]. Similar approaches are the TD-renormalized natural orbital [20] and the TD orbital-adaptive coupled-cluster [21] theories. All these methods are based on a time-dependent optimization of the orbital space, thereby leading to a highly non-linear propagation scheme with convergence issues still under investigation, see also the article by *Hinz et al.* [22] in this volume. The CI expansion on the other hand is based on a time-independent orbital picture and conserves the linearity of the underlying TDSE, although much larger determinantal spaces are required for an accurate description. This deficiency is addressed within the presented TD-GAS-CI approach.

2. Time-dependent generalized-active space configuration interaction

The underlying equation of motion is the time-dependent N -electron Schrödinger equation,

$$i\frac{\partial}{\partial t}|\Psi(t)\rangle = H(t)|\Psi(t)\rangle. \quad (1)$$

with a time-dependent Hamilton operator

$$H(t) = \sum_{i=1}^N t_i + v_i(t) + \sum_{i < j}^N w_{ij}. \quad (2)$$

$t_i \equiv t(\mathbf{r}_i)$ and $v_i \equiv v_{\text{ion}}(\mathbf{r}_i) + E(t)\mathbf{r}_i$ describe the kinetic and potential energies of particle i at position \mathbf{r}_i , and $w_{ij} \equiv w(\mathbf{r}_i, \mathbf{r}_j)$ denotes the interaction between electrons i and j . The excitation with an external field, e.g. a laser, is coupled via the dipole operator in length gauge, \mathbf{r} , with the time-dependent electrical field amplitude $E(t)$. In this contribution, we consider only linear polarization.

2.1. The generalized-active space method

The generalized-active space (GAS) concept to calculate approximate solutions to Eq. (1), as many recently developed methods, is inspired from time-independent quantum chemistry considerations [23, 24]. It is founded on the configuration interaction (CI) expansion of the N -electron wave function,

$$|\Psi_N(t)\rangle = \sum_{I \in \text{GAS}} c_I(t)|I\rangle, \quad (3)$$

where $|I\rangle$ denotes an N -electron Slater determinant constructed from $2N_b$ time-independent single-particle spin orbitals $\chi_i(\mathbf{x}) \equiv \phi_i(\mathbf{r})s(\sigma)$ with $\mathbf{x} = (\mathbf{r}, \sigma)$ referring to the spatial orbital $\phi_i(\mathbf{r})$ and the spin part $s(\sigma)$ with $s \in \{|\uparrow\rangle, |\downarrow\rangle\}$. $c_I(t)$ are the time-dependent complex expansion coefficients. Typically, $|I\rangle$ is constructed from HF orbitals or HF-like pseudo orbitals, which describe the excitations of the system more accurately than common HF virtual orbitals [25].

The basic idea of GAS is the reduction of the exponentially large N -electron Hilbert space to an active subspace, which is capable of describing the physics, but to much less numerical cost than the full CI (FCI) method. This is achieved by partitioning the single-particle space into subspaces with fixed number of electrons. Thereby, it is possible to freeze certain parts of the many-body wavefunction which are unlikely to take part in the dynamics (e.g. by considering energy scales). Details of the idea, technical aspects of the GAS construction and illustrative examples are given in Refs. [25, 26]. A schematic of examples for GAS partitions is drawn in

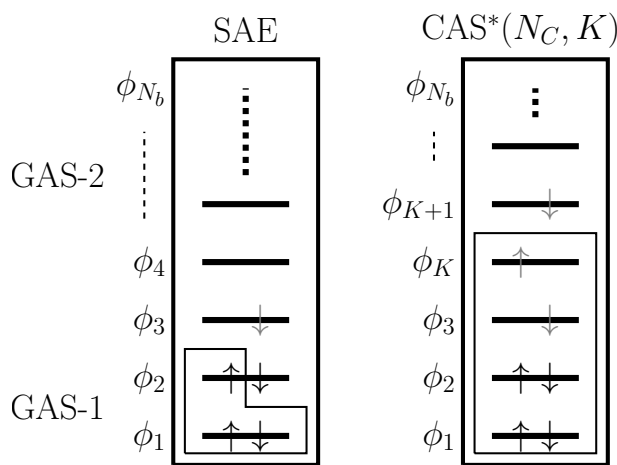


Figure 1. Schematic of GAS definitions for SAE (left) and correlated CAS (right) calculations with four electrons. ϕ_i are the spatial orbitals, which can be occupied by \uparrow and \downarrow electrons. For SAE, three electrons in GAS-1 are frozen and the outer \downarrow electron is allowed to be excited, $i > 2$ (gray arrows). For the CAS, $N_C = 4$ electrons occupy K orbitals in any possible configuration. For $i > K$, only one electron is allowed to occupy higher orbitals. In the picture, the example of \downarrow is sketched (gray arrows indicate excited electrons). In the calculations, every realization is possible.

Fig. 1. The time-dependent realization of GAS-CI was first introduced in the context of time-dependent restricted-active-space (RAS) CI in Ref. [26] and applied to the ionization of helium, beryllium and neon [27]. Throughout, we use the historically motivated acronyms “RAS” and “GAS” as synonyms of the same method. A comprehensive study of convergence and a detailed layout of the method are discussed in [25], further studies using TD-GAS-CI comprise correlation effects in the enhanced-ionization phenomena of molecules [28] and a study of the four-electron LiH molecule in prolate spheroidal coordinates [29]. For more information see also the review article [13].

Within the GAS formalism, several well-established approximation schemes are contained. In this contribution, we will use the single-active electron (SAE), the CI singles (CIS) and special cases of the complete active space (CAS) approximations. For the SAE case, expansion (3) consists only of excitations of one electron with all other $N - 1$ electrons kept frozen in their HF reference orbitals, see Fig. 1 (left) for a schematic of a four-electron system. In contrast to common SAE calculations, no additional pseudo potential needs to be constructed in the GAS framework and all interactions are contained on the same level in the Hamiltonian, Eq. (2). For CIS, the restriction to only one active electron is loosened, and all electrons may be excited, however, only one at a time.

The important CAS case is more involved, as it can be tuned toward the fully converged FCI case containing all electron correlation contributions. We will use the specially adapted notation $CAS^*(N_C, K)$, which corresponds to $N_C \leq N$ electrons occupying $K \ll N_b$ spatial orbitals ($2K$ spin orbitals) and on top of that single-excitations out of the CAS, which is referred to by the $*$ symbol. In this notation, the familiar CIS method is denoted by $CAS^*(N_C, N_C/2)$ [N_C electrons occupy always $N_C/2$ spatial orbitals and one electron may be excited]. Therefore, in the quantum chemistry community, also the term “multi-reference CIS” is widely used for this kind of GAS with $K > N_C/2$. These CAS^* approximations are especially useful for photoionization, as they describe the correlated motion of all (or some) electrons within a subspace and one electron is allowed to occupy every spin orbital, such as continuum states. See Fig. 1 (right) and the corresponding caption for an example. Further information on notations and illustrative examples are provided in Refs. [25, 29].

2.2. Mixed-basis set approach

An essential ingredient to a successful application of truncated CI expansions, i.e., the efficient application of the GAS-CI concept, is a good reference state. Typically in usual CI calculations, the Hartree-Fock (HF) or a similar optimized state is chosen, from which excited Slater

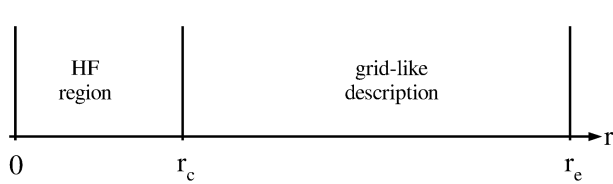


Figure 2. Layout of the mixed basis. Close to the atom or molecule, $r < r_c$, a localized basis (HF-like) is constructed to allow for good CI-reference properties. For $r \geq r_c$, a grid-like representation is employed. For 1d systems, a similar boundary appears for $r < 0$.

determinants are created. However, especially the two-electron integrals in the HF basis comprise a four-indexed object, w_{ijkl} , which prohibits the application for large basis sets because $\mathcal{O}(N_b^4)$ two-electron integrals need to be calculated and stored. Note that N_b is large ($\gg 100$) for photoionization calculations due to the discretized continuum description.

Therefore, we employ a mixed basis set, allowing for an accurate description of the bound part and the scattering states, which combines the best of both worlds: the good reference properties in vicinity to the nucleus and a grid-like discretized continuum with sparse interaction matrices. Technically, a finite-element discrete-variable-representation (FE-DVR) basis is used and partially transformed to a HF-like basis within a central region of the computational grid close to the nuclei, $r < r_c$, see Fig. 2. The great benefit originates from the fact that the two-electron integrals in FEDVR representation, e.g. [30], are extremely sparse, $w_{ijkl} \propto \delta_{ij}\delta_{kl}$, and under the partial rotation, this property is conserved for the largest part of the basis ($r \geq r_c$) [25].

In the context of time-dependent CI calculations, this technique was introduced by *Hochstuhl and Bonitz* in Ref. [26]. The details of the transformation from the full grid to the mixed basis and technical aspects for its efficient implementation are presented and discussed in Ref. [25], the application to atoms in spherical coordinates is addressed in Refs. [26, 27] and in prolate spheroidal coordinates for diatomic molecules in [29]. A similar partitioning technique is also applied in the successful time-dependent R-Matrix theory [31, 32], in a recent formulation even with two-electron continua [33].

3. Application to four-electron molecules

To demonstrate TD-GAS-CI, we consider in the following the four-electron LiH molecule in one spatial dimension and the fixed-nuclei (Born-Oppenheimer) approximation. Hence, only the electronic degrees of freedom are treated in a time-dependent fashion, which is applicable due to the large separation of time scales caused by the large mass differences between the heavy nuclei and the electrons.

3.1. 1d model of LiH

We consider a regularized binding potential for the electrons (R is the internuclear distance, $Z_i \in (1, 3)$ are the nuclear charges) of

$$v_{\text{ion}}(x) = -\frac{Z_1}{\sqrt{(x - R/2)^2 + 1}} - \frac{Z_2}{\sqrt{(x + R/2)^2 + 1}}, \quad (4)$$

and an electron-electron interaction term of

$$w(x_1, x_2) = \frac{1}{\sqrt{(x_1 - x_2)^2 + 1}}, \quad (5)$$

to remove the Coulomb singularities. Such forms of the potentials are well-established models in the literature, see, e.g. Ref. [25] and references therein. A similar model has been used for

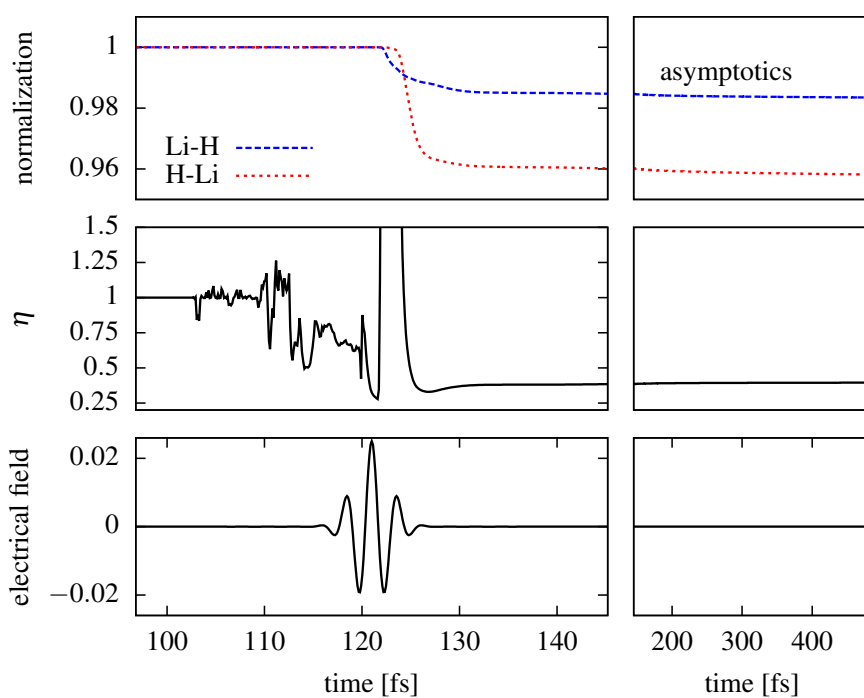


Figure 3. (color online). Normalization of the wave function (top) for both orientations of the LiH molecule with respect to the peak of the electrical field (bottom) and the ionization parameter η , Eq. (8) (center). The asymptotic behavior for long times is shown in the right panels, the dynamics during the pulse in the left panels. Data is for $\tau = 75$ and $E = 0.025$ and $t_0 = 125$ in SAE approximation.

the investigation of enhanced ionization phenomena in molecules, also using the TD-GAS-CI formalism [28].

In such a model, the laser field is polarized along the internuclear axis. Throughout, we consider fields in Eq. (2) of the form

$$E(t) = f(t)E_0 \cos [\omega(t - t_0) + \varphi_{\text{CEP}}] , \quad (6)$$

with a Gaussian-shaped envelope

$$f(t) = \exp [(t - t_0)^2 / (2\tau^2)] . \quad (7)$$

The photon energy is denoted by ω , the maximum field strength by E_0 , which relates to the peak intensity of the field via $I_0[\text{W/cm}^2] = 3.56 \cdot 10^{16} \text{ W/cm}^2 \times E_0^2$. φ_{CEP} denotes the phase between the envelope $f(t)$ and the carrier wave, the pulse duration is given by τ . In the following, we will choose $\varphi_{\text{CEP}} = 0$. Due to the asymmetric potential, Eq. (4), a strong dependence of the orientation w.r.t. to the dominant field cycle is expected [25]. We will denote the configuration $Z_1 = 1, Z_2 = 3$ with Li-H and $Z_1 = 3, Z_2 = 1$ with H-Li. For the former, the direction of the force acting on the electrons due to the external electric field at its maximum [$t = t_0$ in Eq. (7)] points from H to the Li, thus ionization happens from the Li end (and vice versa for the opposite configuration).

3.2. Calculation of ionization yields

To calculate total ionization probabilities, we add a complex absorbing potential (CAP) to the hamiltonian, which is located at the boundary region of the computational box. During the time evolution, the normalization $n(t) = |\langle \Psi(t) | \Psi(t) \rangle|^2$ is therefore not conserved and the absorbed part, $P(t) = 1 - n(t)$, is a measure for the ionization yield. This procedure was introduced by *Kulander* [8]. Details of the employed CAP can be found in Refs. [25, 28].

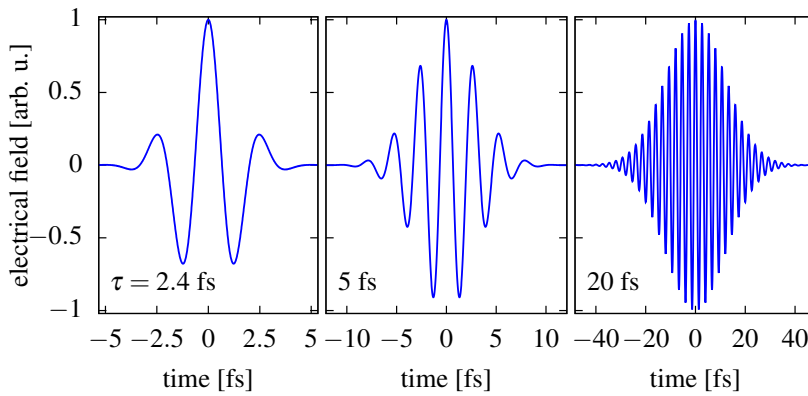


Figure 4. Shape of the Gaussian pulses, Eq. (6), used in this work ($\varphi_{\text{CEP}} = 0$). In the lower corner, the FWHM duration of the intensity ($I(t) \propto E^2(t)$) is printed. The situation $t_0 = 0$ in Eq. (6) is chosen to emphasize the asymmetry of the pulse w.r.t. the sign of the electrical field amplitude.

To investigate the orientation dependence of the ionization yield in our 1d model, we follow Refs. [25, 29] and introduce an orientation parameter

$$\eta = \frac{\mathcal{P}^{\text{H-Li}}(t \rightarrow \infty)}{\mathcal{P}^{\text{Li-H}}(t \rightarrow \infty)}, \quad (8)$$

which describes the ratio of ionization w.r.t. the orientation of the molecule. Values of $\eta < 1$ correspond to a more favourable ionization of Li-H, whereas $\eta > 1$ to H-Li.

To illustrate the methodology, the temporal behavior of the ionization yields are given in Fig. 3 for both orientations of the LiH molecule along with the parameter η for an intermediate electrical field strength $E = 0.025$ (throughout, atomic units are used if not stated otherwise), a pulse duration of $\tau = 75$ (3 fs FWHM of intensity) and using the SAE approximation. After a fast dynamics in the observables during the pulse (left panels), a convergence for large times is found (right panels in the figure), as expected. The ionization probabilities entering in Eq. (8) are extracted from the asymptotic value of the ionization yield, typically at $t > 500$ fs. We checked for convergence of the results with the size of the simulation box, the grid spacing, and the position of the CAP and found no significant variation of the observables.

3.3. Pulse duration

We first turn our attention to the behavior of the ionization parameter η [Eq. (8)] as a function of the pulse duration τ at a fixed electrical field strength of $E_0 = 0.025$, which corresponds to an intensity of 2.2×10^{14} W/cm² and a photon energy of $\omega = 0.057$ (800 nm). By tuning the pulse duration from 2.4 fs to about 40 fs, qualitatively different regimes from single-cycle pulses to long continuous-wave like pulses are covered, see Fig. 4 for an illustration. Due to the asymmetric target molecule and the chosen CEP of the pulse, a strong influence of the orientation of the molecule w.r.t. the peak electrical field strength ($t = 0$ in Fig. 4) is expected for short pulses (left panel), which should vanish for rather long pulses (right panel).

The corresponding ratio of the ionization yield η at different levels of GAS approximations as a function of the pulse duration is given in Fig. 5. Let us first discuss the uncorrelated SAE results (red dotted line). The strongest asymmetry is observed for the shortest pulses ($\tau < 4$ fs), which results from the strong directional character of the single-cycle pulse with one dominant cycle pointing at either the Li or the H nucleus. $\eta < 1$ corresponds to a preferred configuration of ionization of Li-H, which shows in the limit of the shortest possible pulse at $\omega = 0.057$ a factor of five ($\eta \approx 0.2$) higher yields than the configuration H-Li. As expected, an increase of the pulse duration converges η to unity due to the symmetry of the long pulse. The observed convergence is not monotonic but oscillatory with the pulse duration with a period of about 8 fs.

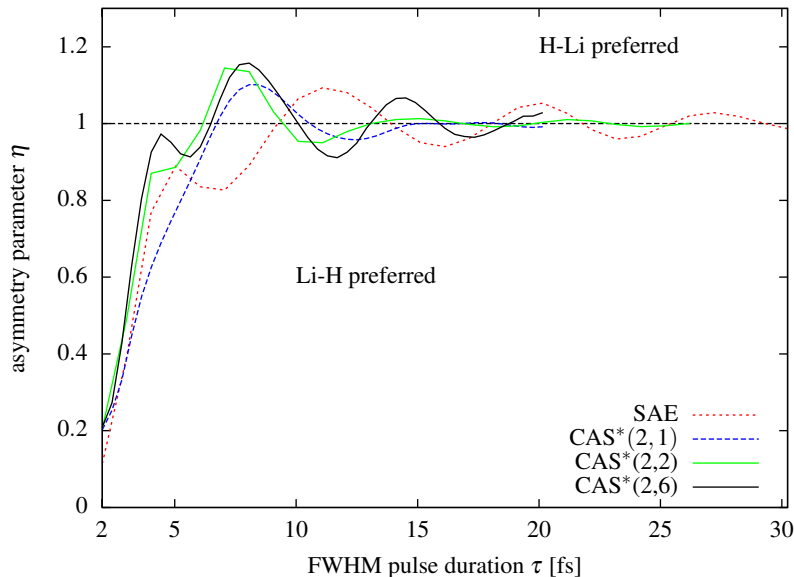


Figure 5. (color online). Ionization parameter η , Eq. (8), as a function of the FWHM pulse duration of the pulse, Eqs. (6), at an electrical field strength of $E_0 = 0.025$ (2.2×10^{13} W/cm 2). $\eta > 1$ ($\eta < 1$) corresponds to a more favourable ionization of H-Li (Li-H).

The reviewed TD-GAS-CI formalism allows us to investigate the influence of electronic correlations. The first improvement is the CAS*(2, 1) [or equivalently TD-CIS, see Sec. 2.1] approximation (blue dashed line), which shows similar behavior as the SAE result, but with a drastic phase shift of the observed oscillations in η . Further inclusion of correlations (green and black solid lines) shifts the oscillations such that the preferred configuration is opposite to that of the uncorrelated SAE calculation (black solid vs. red dashed line). This means that for certain regimes of pulse durations, correlation decides which configuration is easier to ionize and correlated and uncorrelated results are “flipped”.

To check whether this oscillatory behavior is only present at the chosen intensity, we calculated η as a function of the pulse duration for different electric field strength in SAE approximation, see Fig. 6. For small electric fields, only the first minimum is found (red dotted and blue dashed lines) and by successively increasing the intensity more and more pronounced oscillations in the ratio appear. This lets us conclude that the observed structures are especially important at higher intensities.

3.4. Validity of the frozen-core approximation

The above calculations considered only CAS space with two active electrons ($N_C = 2$) thereby freezing the inner shell. This should be a valid scheme since the core level located nearby the lithium atom is much more tightly bound than the valence orbital. Nevertheless, the TD-GAS-CI formalism allows us to test the validity of this frozen core approximation within computational limits. We in the following compare CAS calculation with equivalent sizes, i.e., CAS*(2, K) and CAS*(4, $K + 1$), where the latter include four active electrons.

For the TD-CIS-like calculations, this results in CAS*(2, 1) with a frozen core and two active electrons and CAS*(4, 2) with four active electrons. The results are presented in Fig. 7, and nearly no difference is observed (green fine dotted vs black solid curves) from which we conclude that the frozen-core approximation is valid for the considered regimes of intensity and photon energy. We note, however, that for intense pulses or high photon energies, where inner-shell ionization becomes possible, it is necessary to include the electrons in the dynamics.

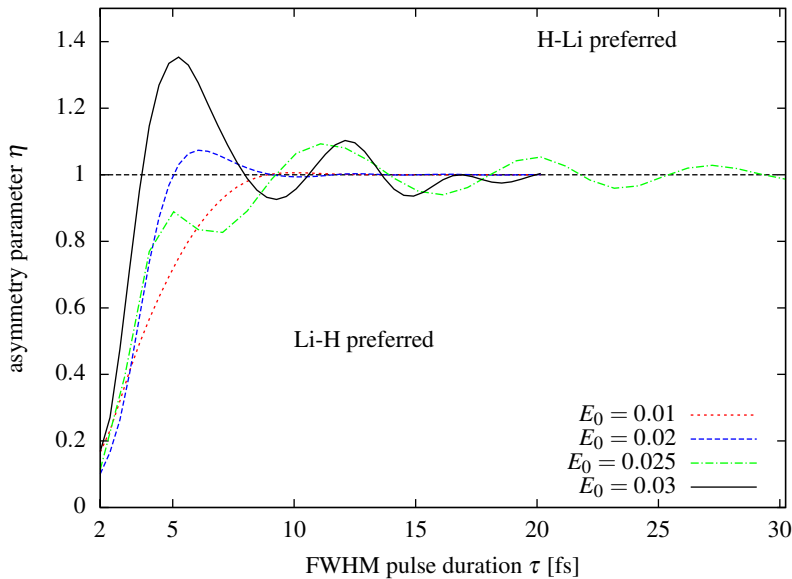


Figure 6. (color online). The same as Fig. 5 but for different pulse intensities at SAE level.

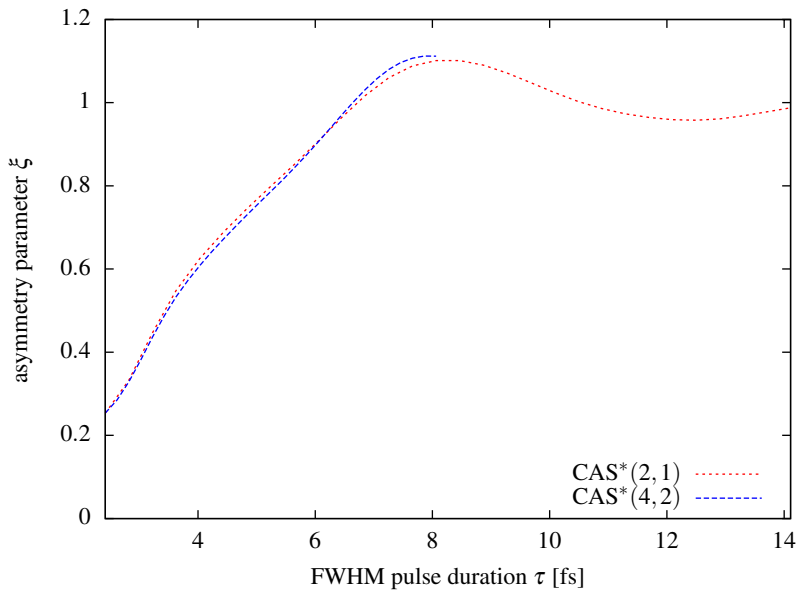


Figure 7. (color online). Comparison of a frozen-core, CAS*(2, 1), and an all-active electrons, CAS*(4, 2), calculation on the CIS level to test for the validity of the frozen-core approximation. Due to the increased computational cost for four active electrons, CAS*(4, 2) is shown only up to 8 fs.

4. Conclusions

In this contribution, we reviewed the time-dependent generalized active space configuration interaction (TD-GAS-CI) approach to the photoionization of atoms and molecules. We introduced the basic idea of selecting important Slater determinants in the CI expansion and addressed the mixed basis set as an essential ingredient to a numerically tractable scheme. We then demonstrated the theory by applying it to the ionization of a heteronuclear 1d model molecule in a strong field with its strongest peak pointing in one direction. For such an excitation scenario the total ionization yields of the two possible orientations in one spatial dimension have been compared and strong influences of electronic correlations have been found. Even the opposite configuration w.r.t. the electric peak for correlated vs. uncorrelated calculation can be found. Ongoing work is in the direction of 3d molecules and larger systems. One possible approach by means of a prolate spheroidal basis is pursued in Ref. [29], with the focus on the

3d LiH molecule. Following these extensions of the TD-GAS-CI theory, it will become possible to validate the presented correlation-driven observations of a one-dimensional model in more realistic systems which can then be tested by experiment.

Acknowledgments

The authors gratefully acknowledge funding by the German Federal Ministry for Education and Research in the frame of the Verbundprojekt "FSP-302" and computing time at HLRN via grants shp00006 and shp00013.

- [1] Brabec T and Krausz F 2000 *Reviews of Modern Physics* **72** 545–591
- [2] Schütte B, Bauch S, Fröhling U, Wieland M, Gensch M, Plönjes E, Gaumnitz T, Azima A, Bonitz M and Drescher M 2012 *Physical Review Letters* **108** 253003
- [3] Bauch S and Bonitz M 2012 *Physical Review A* **85** 053416
- [4] Schultze M, Fieß M, Karpowicz N, Gagnon J, Korbman M, Hofstetter M, Neppel S, Cavalieri A L, Komninos Y, Mercouris T, Nicolaides C A, Pazourek R, Nagele S, Feist J, Burgdörfer J, Azzeer A M, Ernstorfer R, Kienberger R, Kleineberg U, Goulielmakis E, Krausz F and Yakovlev V S 2010 *Science* **328** 1658–1662
- [5] Überacker M, Uphues T, Schultze M, Verhoef A J, Yakovlev V, Kling M F, Rauschenberger J, Kabachnik N M, Schröder H, Lezius M, Kompa K L, Muller H G, Vrakking M J J, Hendel S, Kleineberg U, Heinzmamn U, Drescher M and Krausz F 2007 *Nature* **446** 627–632
- [6] Kling M F and Vrakking M J 2008 *Annu. Rev. Phys. Chem.* **59** 463–492
- [7] Krausz F and Ivanov M 2009 *Reviews of Modern Physics* **81** 163–234
- [8] Kulander K C 1987 *Physical Review A* **35** 445–447
- [9] Krause J L, Schafer K J and Kulander K C 1992 *Physical Review Letters* **68** 3535–3538
- [10] Taylor K T, Parker J S, Dundas D, Meharg K J, Doherty B J S, Murphy D S and McCann J F 2005 *Journal of Electron Spectroscopy and Related Phenomena* **144–147** 1191–1196
- [11] Parker J S, Doherty B J S, Taylor K T, Schultz K D, Blaga C I and DiMauro L F 2006 *Physical Review Letters* **96** 133001
- [12] Bauch S, Balzer K and Bonitz M 2010 *EPL (Europhysics Letters)* **91** 53001
- [13] Hochstuhl D, Hinz C M and Bonitz M 2014 *The European Physical Journal Special Topics* **223** 177–336
- [14] Meyer H D, Manthe U and Cederbaum L S 1990 *Chemical Physics Letters* **165** 73–78
- [15] Hochstuhl D, Bauch S and Bonitz M 2010 *Journal of Physics: Conference Series* **220** 012019
- [16] Hochstuhl D and Bonitz M 2011 *The Journal of Chemical Physics* **134** 084106–084106–10
- [17] Miyagi H and Madsen L B 2013 *Physical Review A* **87** 062511
- [18] Sato T and Ishikawa K L 2013 *Physical Review A* **88** 023402
- [19] Sato T and Ishikawa K L 2015 *Physical Review A* **91** 023417
- [20] Brics M and Bauer D 2013 *Physical Review A* **88** 052514
- [21] Kvaal S 2012 *The Journal of Chemical Physics* **136** 194109
- [22] Hinz C, Bauch S and Bonitz M 2015 *J. Phys.: Conf. Ser.: this volume*
- [23] Olsen J, Roos B O, Jørgensen P and Jensen H J A 1988 *The Journal of Chemical Physics* **89** 2185–2192
- [24] Sørensen L K, Fleig T and Olsen S 2010 *Zeitschrift für Physikalische Chemie International journal of research in physical chemistry and chemical physics* **224** 671–680
- [25] Bauch S, Sørensen L K and Madsen L B 2014 *Physical Review A* **90** 062508
- [26] Hochstuhl D and Bonitz M 2012 *Physical Review A* **86** 053424
- [27] Hochstuhl D and Bonitz M 2013 *Journal of Physics: Conference Series* **427** 012007
- [28] Chattopadhyay S, Bauch S and Madsen L B 2015 *arXiv:1508.01629*, accepted for publication in *Phys. Rev. A* (2015)
- [29] Larsson H R, Bauch S and Bonitz M 2015 *arXiv:1507.04107*
- [30] Balzer K, Bauch S and Bonitz M 2010 *Physical Review A* **81** 022510 URL <http://link.aps.org/doi/10.1103/PhysRevA.81.022510>
- [31] van der Hart H W, Lysaght M A and Burke P G 2007 *Physical Review A* **76** 043405
- [32] Lysaght M A, van der Hart H W and Burke P G 2009 *Physical Review A* **79** 053411
- [33] Wragg J, Parker J S and van der Hart H W 2015 *Physical Review A* **92** 022504